# VALIDATION OF AN ORGANIC RANKINE CYCLE MODEL OF A GEOTHERMAL POWER PLANT

Matthew J Proctor, Wei Yu*, and Brent R Young

Department of Chemical and Materials Engineering, Faculty of Engineering, The University of Auckland, New Zealand

*Corresponding Author

mpro027@aucklanduni.ac.nz
w.yu@auckland.ac.nz
b.young@auckland.ac.nz

**Keywords:** *Organic Rankine cycle, process modelling, model validation.*

## ABSTRACT

The Organic Rankine cycle (ORC) has attracted attention around the world over the last decade as a solution to some of the problems posed by climate change and energy scarcity. It is generally accepted that modelling can significantly help engineers with process design, process control, trouble-shooting etc. Both steady state and dynamic models for the ORC processes have been built using the commercial process simulator: VMGSim. These models can be used for the further investigation of optimization and process control. Before these models can be used however, model validation must be conducted. In this paper, we will use white-box and black-box validation methods to validate a preheating heat exchanger and the plant-wide dynamic ORC model.

## 1. INTRODUCTION

The market potential for above ground technology in geothermal and waste heat low enthalpy resources is significant and Organic Rankine Cycle (ORC) technology has been identified as a key energy conversion system for the "green" production of power.

A wide range of ORC applications have been investigated for many heat resources, such as waste heat recovery (Kanoglu 709-724; Schuster et al. 1809-1817; Ozturk et al. 1415-1424) [1-3], geothermal systems [4], solar energy use [5], combined heat and power [6] and engine exhaust gases [7, 8]. More comprehensive literature reviews are provided by Gnuteck and Bryszewska-Mazurek [9] and Kaplan [10].

Our research group, the Industrial Information and Control Centre, has become a part of a big New Zealand geothermal project to design an optimal control system. To fulfil this goal, a model of a geothermal power plant with an Organic Rankine Cycle has been built using a commercial process simulator, VMGSim. The model can also be used for understanding the processes inside a geothermal plant and assist to improve their energy effectiveness

In this paper the validation of a model of a geothermal power plant using an ORC is presented. This validation is divided into two parts: black-box plant-wide validation and white-box validation of the heat exchanger model. For plant-wide validation the output of the model is compared to real data from the plant when the model is run with the same input conditions, for the heat exchanger validation the output from one of the heat exchangers used in the plant model is compared with a more sophisticated model that is derived from an analysis of the underlying heat transfer principles.

The plant-wide model built in VMGSim uses heat exchangers where the overall heat transfer coefficient is set at a constant value. This is potentially an oversimplification as the convective heat transfer coefficients on the geothermal fluid side of the heat exchangers should vary significantly with the different flow regimes and non-condensable gas concentrations of the geothermal fluid. There is also a possibility that the convective heat transfer coefficient on the working fluid side of the heat exchanger will exhibit similar variability. This paper seeks to quantify the difference between a more sophisticated heat exchanger model and the current, simpler models being used in the plant model in order to establish under what conditions and purposes the existing model is "good enough" and whether the additional computational and human effort needed to incorporate a more sophisticated heat exchanger model in the plant-wide model is worthwhile.

The paper is organised as follows: The plant-wide ORC process under investigation is presented along with the methods used to model both the entire plant and a particular heat exchanger using heat transfer principles. The methods for validating the plant-wide model and the heat exchanger are then given. The results of this validation are then presented and discussed followed by the conclusions that can be drawn from the validation.

## 2. ORGANIC RANKINE CYCLE

Geothermal power plants can be broadly divided into two categories: those that use the geothermal fluid in the turbine to generate power and those that use a secondary working fluid into which heat is transferred by the geothermal fluid, known as ORC plants. The first category can be divided into flash plants, which flash the geothermal fluid to get a higher vapour fraction for the turbine and dry steam plants, which use the geothermal fluid directly.

Figure 1 shows the process flow diagram of an ORC system using some heat sources. In the process, hot fluid is used to preheat and vaporise an organic working fluid in the vaporiser. The vapour then passes through a turbine which will turn a shaft connected to a generator to generate electricity. The low pressure organic working fluid vapour from the turbine is then passed through a condenser where it is condensed to liquid using cold water or air. The liquid organic working fluid is then pumped back to the vaporiser to complete the cycle.

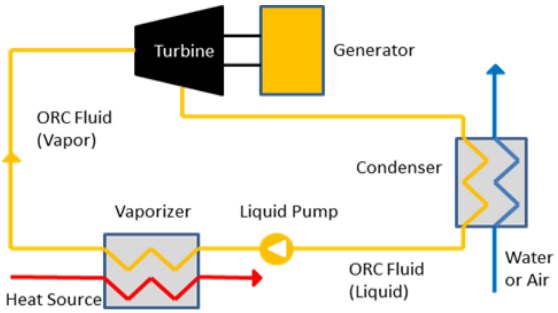


**Figure 1: A schematic of an organic Rankine cycle**

A design incorporating an ORC can use heat sources with lower enthalpy than other geothermal plant designs because it uses a separate working fluid with a lower boiling point. It is not constrained by the rule that the fluid that flows through the turbine must have the same composition as the geothermal fluid. In fact, the working fluid composition is an extra variable can be tailored precisely to the heat source in order to optimise the design in terms of efficiency, capital cost, etc.

## 3. ORC MODELLING

A study of the literature in ORC modelling reveals that the general approach is to model the system using partial/ordinary differential and algebraic equations representing the underlying thermodynamic relationships and mass and energy balances. This is the approach seen in virtually every paper on ORC modelling. Good examples of this approach are seen in [11-13]. One apparent exception to this approach is seen in [14], which uses a transfer function model. However this model is in turn based on an existing dynamic ORC model developed by some of the same authors and shown in [15].

### 3.1 Modelling using VMGSim

The plant-wide dynamic model was built by connecting together pre-built unit operations present in the VMGSim simulator. These included heat exchangers, pumps, expanders, separators, valves and controllers. These unit operations were connected together in the appropriate order to build a model of an existing ORC plant. A screenshot from VMGSim showing the model layout can be seen in Figure 2.

The specifications for the model were based on design temperature, pressure and flow values in the plant documentation. For the heat exchangers this includes pressure drop and overall heat transfer coefficient values (UA values), for the pump the performance curves from the plant documentation (head vs. flow and efficiency vs. flow) were imported into VMGSim, the expander performance curve was not available and so a built-in curve already available in VMGSim was used and PID controllers for the primary control loops were implemented in the model with the same tuning parameters (gain, integral time and derivative time) as the real plant. An air cooler unit operation with built-in relationships for fan power and air flow is not available in VMGSim and so a heat exchanger unit operation was adapted for this purpose. The use of the heat exchanger unit operation present in VMGSim as an air cooler should be validated in the future to determine if it can adequately model a real air cooler.

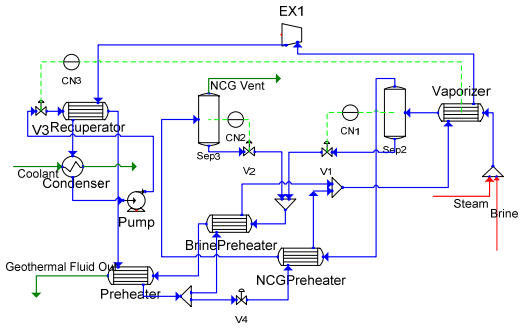


**Figure 2. ORC model in VMGSim.**

### 3.2 Modelling of heat exchangers within ORCs

One area where there is some variation in the ORC models presented in the literature is how heat exchangers are modelled, particularly their heat transfer coefficients. Some papers, such as [16, 17] take a comprehensive approach to determining the heat transfer coefficients based on the underlying heat transfer mechanisms. Others calculate the heat transferred directly using pinch analysis [18] or uses predefined heat transfer rates from existing systems [13]. Other papers do not supply information about heat transfer coefficients, and could be using constant overall heat transfer coefficients in their models, an example being the model being validated in this paper.

In order to construct an accurate heat transfer model it is necessary to examine the literature on heat transfer for the conditions found in the plant's heat exchangers. The non-condensable gas (NCG) preheater was chosen for a more detailed analysis so it could be compared to the simpler model used in the overall plant model. On the working fluid side of the heat exchanger there is liquid phase sensible heating under turbulent conditions and on the geothermal side of the heat exchanger there is two component two phase condensing under stratified two phase flow conditions.

An ideal convective heat transfer coefficient for the shell side of the heat exchanger was calculated, which does not take flow that bypasses the tube bundle into account. The method used for the calculation was taken from [19] and the relevant equations are:

$$\alpha = j_I c_p \dot{\varphi}_m Pr^{-2/3} \quad (1)$$

$$j_I = a_1 \left(\frac{1.33}{L_{tp}/d_i}\right)^a Re^{a_2} \quad (2)$$

$$a = \frac{a_3}{1+0.14Re^{a_4}} \quad (3)$$

$$\dot{\varphi}_m = \frac{\dot{m}}{S_m} \quad (4)$$

$$S_m = L_{bc}\left[L_{bb} + \frac{D_{ctl}}{L_{tp}}\left(L_{tp}/d_i\right)\right] \quad (5)$$

$$Re = \frac{d_i \dot{\varphi}_m}{\mu} \quad (6)$$

$$Pr = \frac{c_p \mu}{k} \quad (7)$$

The definitions of the symbols is as follows: For the inputs to these equations, $L_{tp}$ is the tube pitch, $d_i$ is the tube diameter, $\dot{m}$ is the mass flow rate, $L_{bc}$ is the baffle spacing, $L_{bb}$ is the twice the gap between the tubesheet and shell wall, $D_{ctl}$ is the centreline tube limit diameter, $\mu$ is the shear

viscosity of the fluid in the shell, $c_p$ is the constant pressure heat capacity of the fluid and $k$ is the thermal conductivity of the fluid.

For the outputs and intermediaries for these equations, $\alpha$ is the convective heat transfer coefficient, $S_m$ is the cross-flow area at the bundle centreline, $\dot{\varphi}_m$ is the mass flux, $Re$ is the Reynolds number of the fluid, $Pr$ is the Prandtl number of the fluid, $j_I$ is a correction factor used for the ideal calculation with no bypassing flow, the $a$ values are all empirical coefficients based on Reynolds number and tube layouts. For the NCG preheater at design conditions these were: $a_1 = 0.321$, $a_2 = -0.388$, $a_3 = 1.45$ and $a_4 = 0.519$.

The Reynolds and Prandtl numbers are calculated at the mean temperature of the fluid in the shell and therefore the convective heat transfer coefficient on this side of the heat exchanger remains constant along the length of the exchanger.

For the tubes, a constant thermal conductivity of $50.2\ W/m.K$ was taken from (ref University Physics) as a typical value for steel.

A series of convective heat transfer coefficients were calculated for geothermal fluid on the tube side of the heat exchanger. The heat exchanger was divided into five segments and a heat transfer coefficient was calculated for each segment based on the Thome-El Hajal-Cavallini method also given in [19]. The relevant equations are:

$$\boldsymbol{\varepsilon = \frac{\varepsilon_H - \varepsilon_r}{\ln(\varepsilon_H/\varepsilon_r)}} \quad \textbf{(8)}$$

$$\boldsymbol{\varepsilon_H = \frac{1}{1+\left(\frac{1-x}{x}\right)\frac{\rho_G}{\rho_L}}} \quad \textbf{(9)}$$

$$\boldsymbol{\varepsilon_r = \frac{x}{\rho_G}\left(\left[1 + 0.12(1-x)\left[\frac{x}{\rho_G}+\frac{1-x}{\rho_L}\right] + \frac{1.18(1-x)[g\sigma(\rho_L-\rho_G)]^{0.25}}{\dot{\varphi}_m \rho_L^{0.5}}\right]\right)^{-1}} \quad \textbf{(10)}$$

$$\boldsymbol{\theta_{strat} =}$$

$$\boldsymbol{2\pi - 2\left\{\begin{array}{c}\pi(1-\varepsilon) + \left(\frac{3\pi}{2}\right)^{1/3} \\ \times\left[1 - 2(1-\varepsilon) + (1-\varepsilon)^{1/3} - \varepsilon^{1/3}\right] \\ -\frac{1}{200}(1-\varepsilon)\varepsilon[1-2(1-\varepsilon)] \\ \times\left[1+4\left((1-\varepsilon)^2+\varepsilon^2\right)\right]\end{array}\right\}} \quad \textbf{(11)}$$

$$\boldsymbol{\alpha_c = cRe_L^n Pr_L^m \frac{k_L}{\delta} f_i} \quad \textbf{(12)}$$

$$\boldsymbol{Re_L = \frac{4\varphi_m(1-x)\delta}{(1-\varepsilon)\mu_L}} \quad \textbf{(13)}$$

$$\boldsymbol{Pr_L = \frac{c_{pL}\mu_L}{k_L}} \quad \textbf{(14)}$$

$$\boldsymbol{A_L = (1-\varepsilon)A} \quad \textbf{(15)}$$

$$\boldsymbol{A_L = \frac{(2\pi - \theta_{strat})}{8}\left[d_i^2 - \left(d_i^2 - 2\delta\right)^2\right]} \quad \textbf{(16)}$$

$$\boldsymbol{u_L = \frac{\dot{\varphi}_m(1-x)}{\rho_L(1-\varepsilon)}} \quad \textbf{(17)}$$

$$\boldsymbol{u_G = \frac{\dot{\varphi}_m x}{\rho_G \varepsilon}} \quad \textbf{(18)}$$

$$\boldsymbol{f_i = 1 + \left(\frac{u_G}{u_L}\right)^{1/2}\left(\frac{(\rho_L-\rho_G)g\delta^2}{\sigma}\right)^{1/4}\left(\frac{\dot{\varphi}_m}{\dot{\varphi}_{m,strat}}\right)} \quad \textbf{(19)}$$

$$\boldsymbol{\alpha_f = 0.655\left[\frac{\rho_L(\rho_L-\rho_G)gh_{vap}k_L^3}{\mu_L d_i q}\right]^{\frac{1}{3}}} \quad \textbf{(20)}$$

$$\boldsymbol{\alpha = \frac{\alpha_f\theta_{strat} + (2\pi - \theta_{strat})\alpha_c}{2\pi}} \quad \textbf{(21)}$$

The definitions of the symbols in these equations are: $L$ and $G$ subscripts refer to liquid and gas respectively, $x$ is the vapour fraction on a mass basis, $\rho$ is the density, $c$, $n$ and $m$ are empirical coefficients that are equal to 0.5, 0.74 and 0.003 respectively, $\varepsilon$ is the void fraction, $\varepsilon_H$ is the homogenous void fraction, $\varepsilon_r$ is the Rouhani void fraction, $g$ is the gravitational acceleration, $\sigma$ is the surface tension between liquid and vapour, $\delta$ is the thickness of the stratified liquid layer running along the bottom of the tube, $A_L$ is the cross sectional area of this liquid layer, $A$ is the cross sectional area of the entire tube, $u$ is the velocity of the fluid, $f_i$ is a correction factor that takes the roughness between the liquid annular film around the tube and the vapour flow into account, $\dot{\varphi}_{m,strat}$ is the critical mass flux at the transition from the stratified flow to stratified-wavy flow regime, $h_{vap}$ is the heat of vaporisation (mass basis), $q$ is the heat flux, $\theta_{strat}$ is twice the angle between the liquid stratified layer and the top of the tube, $\alpha_c$ is the convective heat transfer coefficient for the annular liquid film, $\alpha_f$ is the convective heat transfer coefficient for the stratified liquid flow and $\alpha$ is the overall heat transfer coefficient.

As in the previous set of equations $k$ is the thermal conductivity, $c_p$ is the constant pressure heat capacity, $Re$ is the Reynolds number, $Pr$ is the Prandtl number, $\dot{\varphi}_m$ is the mass flux and $d_i$ is the tube diameter.

The Thome- El Hajal-Cavallini method becomes more sophisticated when more liquid is present in the flow as the more complex two phase flow regimes require more detailed analysis. The set of equations given above are for fully stratified flow which occurs at the high void fractions present in the NCG preheater. This method does not take into account the effect of a non-condensable gas. The effect of non-condensable gas on the condensing heat transfer coefficient is discussed in [20], but only for the shell side of a heat exchanger. He notes that non-condensable gases will cause lower heat transfer coefficients due to the formation of a film through which condensable vapour will have to diffuse before reaching the condensing surface. Therefore it should be expected that the heat transfer coefficients found for the tubes in the NCG preheater will be higher than in reality.

Using a thermal resistance model, the overall heat transfer coefficient for the NCG preheater was calculated:

$$\boldsymbol{\frac{1}{U} = \frac{1}{\alpha_{tubes}} + \frac{\Delta x}{kA} + \frac{1}{\alpha_{shell}}} \quad \textbf{(22)}$$

With $U$ being the overall heat transfer coefficient, $\Delta x$ being the tube wall thickness, $A$ being the area of the tubes and $k$ being the thermal conductivity of the tubes. This was then multiplied by the area of the tubes to calculate the UA value, which was then used to calculate the heat transferred in each segment:

$$\boldsymbol{\dot{Q} = U \cdot A \cdot \Delta T} \quad \textbf{(23)}$$

Where $\Delta T$ is the difference in temperature between the fluid in the shell and in the tubes.

## 4. MODEL VALIDATAION

Before a simulation model can be used for any purpose, we must ask a simple question: is the model valid? If a model is not valid, then any results based on the model will be unreliable. There two significant concerns for any simulation are verification and validation (V&V). Definitions for V&V are given in the classic simulation text book [21] as "*verification* is determining that a simulation computer program performs as intended, i.e., debugging the computer program…. *validation* is concerned with determining whether the conceptual model (as opposed to the computer program) is an accurate representation of the system under study". The conceptual model of a process is a formal definition of the system under consideration in logical or mathematical form, typically comprising the underlying theoretical equations. In this paper, we will only focus on the validation of our models. The fundamental concepts and theories about verification and validation of simulation models can be found in [21-23].

Four methods for model validation proposed by [24] are: conceptual model validation, data validation, white-box validation and black-box validation. The interplay between these validation methods during the modelling processes is shown in [24]. In this paper, we will only use two model validation methods: white-box validation and black-box validation. White-box validation focuses on checking that the individual components in a model correspond to reality. In black-box validation the overall behaviour of the model is evaluated. The same inputs which enter the real processes or systems will be tested on the model, the outputs from the real processes or systems and the model will be compared.

VMGSim simulation software is the platform for ORC modelling; the existing unit operations present in the software have not been validated since this has already been done by the software developer. However some of these unit operations may not be able to properly model the ORC plant under consideration. Using the white-box validation method, we will check whether the heat exchangers can adequately model the real units, using the NCG preheater as a test case. For the black-box validation, the outputs from the real ORC plant (historical plant data) under consideration will be compared to model outputs for the same set of input conditions.

### 4.1 White-box Validation

For the white-box validation, the NCG preheater was modelled in VMGSim at design conditions by dividing it into five horizontal segments in sequence. The method described in section 3.2 was then applied to each segment, using the physical properties of the fluid present in VMGSim. Using the new values for the heat transferred in the sections, new outlet temperatures were calculated for the NCG stream within each segment of the NCG heat exchanger and these temperatures were contrasted with the results from VMGSim. The temperatures are presented in Table 1.

**Table 1. NCG Output Temperatures for the VMGSim and principles-based models.**

| Segment | New Model NCG Output Temperature (°C) | VMGSim NCG Output Temperature (°C) | Absolute Difference (°C) |
|---|---|---|---|
| 1 | 167.95 | 165.82 | 2.13 |
| 2 | 161.63 | 160.84 | 0.79 |
| 3 | 152.10 | 153.52 | 1.42 |
| 4 | 136.48 | 141.96 | 5.48 |
| 5 | 113.42 | 122.00 | 8.58 |

From the results it can be seen that there is a difference between assuming a constant heat transfer coefficient and calculating it from heat transfer principles. For this particular heat exchanger the difference is smaller for higher NCG temperatures, but as the NCG stream becomes cooler the absolute temperature difference increases. The difference between output from VMGSim and the more fundamental model is expected to be even greater when the NCG preheater is not operating at design conditions as factors such as different two phase flow regimes will cause the calculated heat transfer coefficient to deviate even further from the constant VMGSim coefficient.

### 4.1 Black-box Validation

For the black-box validation, the plant-wide model created in VMGSim was run using 800 minutes of real historical plant data as the input. Certain output variables that are monitored in the real plant were recorded from VMGSim and compared to the same output variables from the historical plant data.

The inputs into the VMGSim model were the steam temperature, brine temperature, steam mass flow rate, brine mass flow rate and the ambient temperature, which is modelled in VMGSim as the temperature of the coolant running through the condenser. The output variables were the vaporiser percentage liquid level, the turbine power output and the working fluid temperature outputs of all six heat exchangers (preheater, brine preheater, NCG preheater, vaporiser, condenser and recuperator).

Plots of the inputs into the model are presented below:

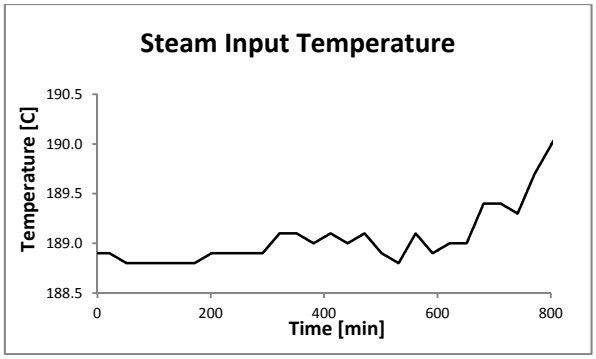


**Figure 3. Input values for the steam temperature.**

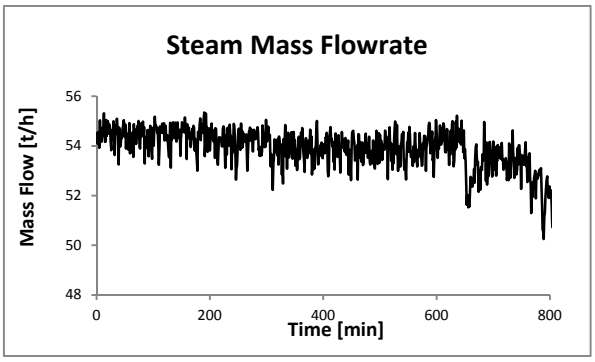


**Figure 4. Input values for the steam mass flowrate.**

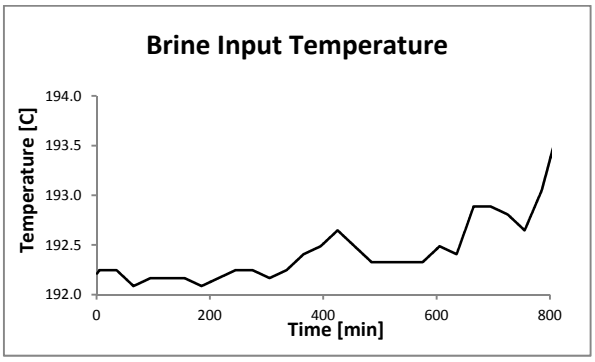


**Figure 5. Input values for the brine temperature.**

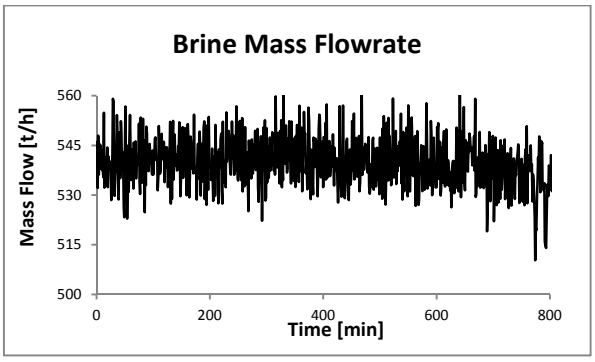


**Figure 6. Input values for the brine mass flowrate.**

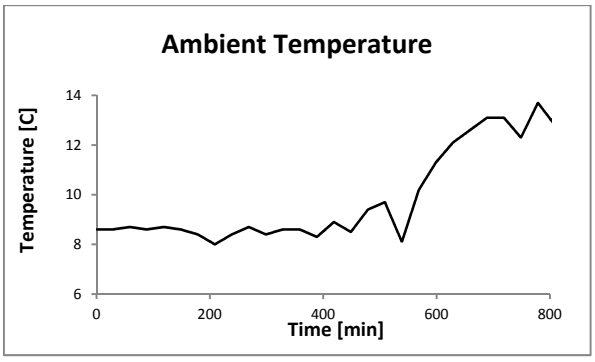


**Figure 7. Input values for the ambient temperature.**

A plot of the residuals for each of the output variables, except for the vaporiser level is presented below. The vaporiser level is not included because its value dropped to zero at the beginning of the simulation. This is most likely due to the model being run using real plant data that does not match the design conditions precisely, and this difference combined with assuming a constant heat transfer coefficient resulted in the liquid working fluid being immediately evaporated upon entering the vaporiser, which is contrary to the real data.

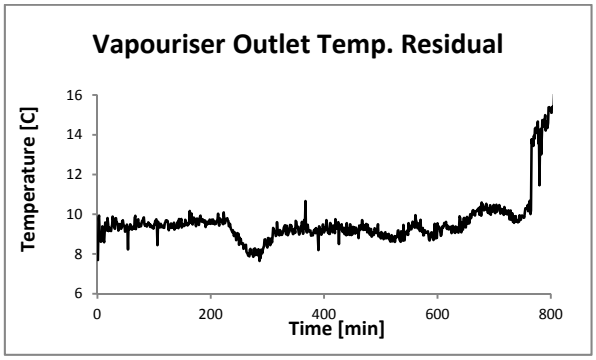


**Figure 8. Residual values for the vaporiser outlet temperature.**

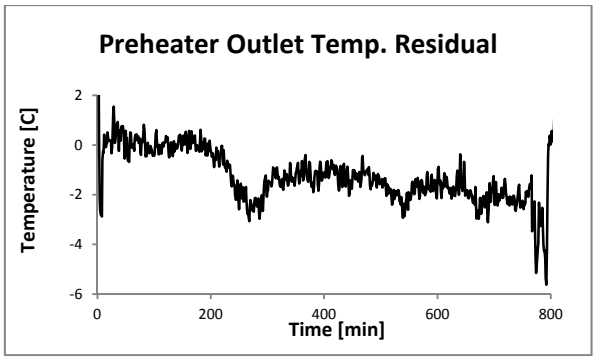


**Figure 9. Residual values for the preheater outlet temperature.**

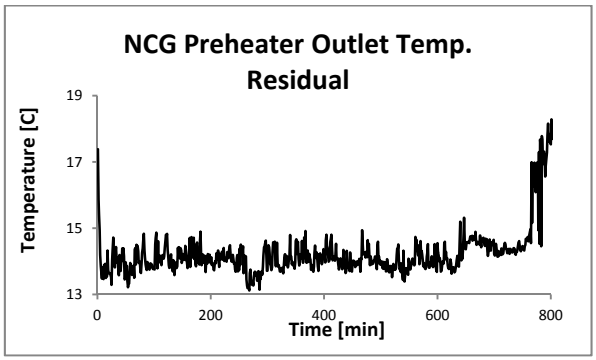


**Figure 10. Residual values for the NCG preheater outlet temperature.**

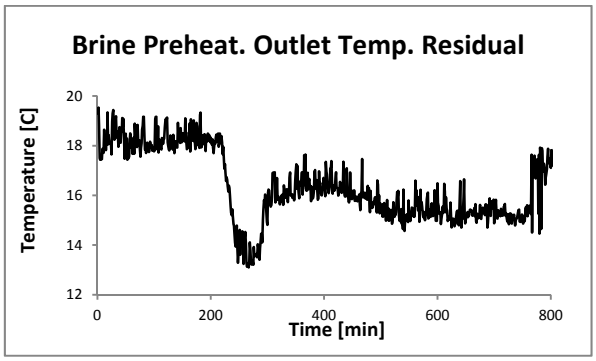


**Figure 11. Residual values for the brine preheater outlet temperature.**

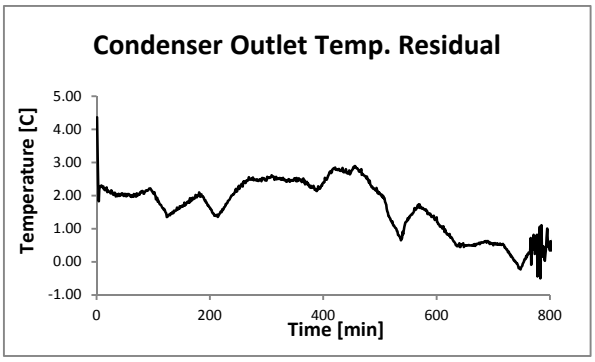


**Figure 12. Residual values for the condenser outlet temperature.**

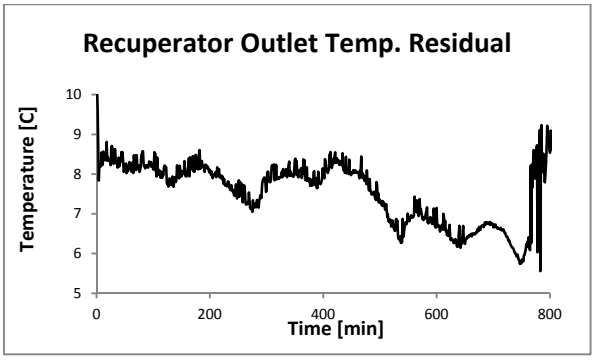


**Figure 13. Residual values for the recuperator outlet temperature.**

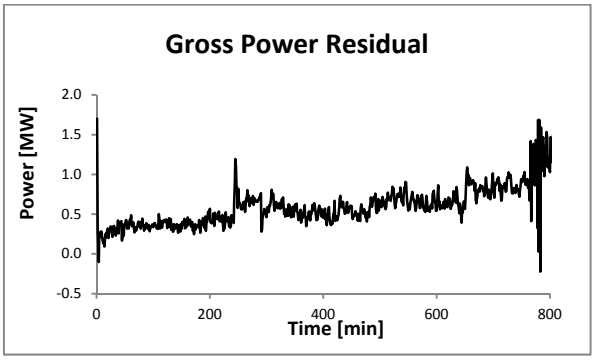


**Figure 14. Residual values for the gross power output.**

An examination of the residual values for the heat exchangers (Figure 8 through to Figure 13) shows that, except for the preheater, the outlet temperature of the working fluid is higher than in reality. The brine preheater shows the largest residuals close to 20 °C, followed by the NCG preheater with around 14 °C, the vaporiser with around 10 °C, the condenser with up to 3 °C and the preheater which had a lower temperature than the real data by 2 °C. This indicates that for the given input conditions assuming constant heat transfer coefficients based on design data tends to overestimate the heat transfer coefficient. These differences will also affect the accuracy of the power output prediction; residual values for power output up to 1 MW can be seen in Figure 14.

At around 750 minutes, all of the residual plots exhibit extra variation. This is caused by the model data; the real data remains relatively constant. It is not completely clear what caused this effect, although the flow of steam and brine into the model does reduce around this time, as can be seen in Figure 4 and Figure 6, and the temperature of the steam and brine rises, as can be seen in Figure 3 and Figure 5. Two potential causes are the heat exchanger models and the control system model. Since the control system model matches the real control system relatively closely as both are based on fairly simple PID equations and the only observable change in the inputs that occurs around this time are changes in the temperatures and flowrates of the input streams to the vaporiser it is reasonable to assume that the cause of this extra variation is also the overly simplistic heat exchanger models.

**Table 2. Statistical summary of the results from the black-box validation.**

| | Mean Real Value | Mean Residual | Standard Deviation of Residual |
|---|---|---|---|
| **Vaporiser Outlet T [C]** | 161.03 | 9.79 | 1.60 |
| **NCG Preheater Outlet T [C]** | 151.70 | 14.36 | 0.95 |
| **Brine Preheater Outlet T [C]** | 149.64 | 16.39 | 1.40 |
| **Preheater Outlet T [C]** | 92.84 | -1.27 | 1.14 |
| **Condenser Outlet T [C]** | 27.70 | 1.62 | 0.83 |
| **Recuperator Outlet T [C]** | 53.67 | 7.60 | 0.79 |
| **Gross Power Output [MW]** | 16.84 | 0.62 | 0.27 |

Table 2 shows a summary of the results from the black-box validation. By contrasting the mean value of the residuals against the mean of the real values it is possible to gain some idea of how well the model approximates the real plant. The ratio of the mean residual to the mean real value for each individual heat exchanger cannot be used as a metric to attribute inaccuracy to the sub-model of that unit alone because they are all closely connected together in a system and inaccuracies in one unit will affect the others. The gross power output ratio of 0.04 (2 d.p), could be considered as the most generally useful ratio since the power output of an ORC is of significant importance commercially.

Whether or not the value of 0.04 is acceptable or not would depend on the level of uncertainty the model's users would be willing to accept, which would depend on their intended application for the model. Similarly, assessment of the ratio for any individual heat exchanger is dependent on the end to which the model is going to be applied. If the model is being used to investigate design options for the brine preheater, for example, then its ratio would be important and whether or not it is considered high or low would also depend on the level of uncertainty that is acceptable in the model's application.

The standard deviation of the residuals gives an indication of how well the model responded to changing conditions. This is because the black-box validation of the model involved exposing it to real plant data that varied over time. If the model was able to account for this variation then the residuals would remain more or less constant and the standard deviation would be low. Higher standard deviations must then indicate that the variations are not taken into account by the model. As with the ratios

mentioned above judgement of these standard deviations must consider the circumstances of a particular application of the model.

## 5. CONCLUSIONS

A fundamental analysis of the heat transfer principles within a heat exchanger inside an ORC plant revealed a difference in the temperature of the heating fluid throughout the heat exchanger of up to 8.5 °C when using calculated heat transfer coefficients compared to assuming constant coefficients determined from design data.

Black-box validation of a plant-wide model revealed differences between real data and model output, particularly higher temperatures in the heat exchangers of up to 20 °C.

These discrepancies impacted the predicted power output of the plant which had residuals of up to 1 MW.

Peculiar variations in the model output were observed around 750 minutes that can be reasonably attributed to overly simplistic heat exchanger models.

## ACKNOWLEDGEMENTS

The authors would like to acknowledge the Heavy Engineering Research Association of New Zealand for their support of this research.

## REFERENCES

1. Kanoglu, M., *Exergy analysis of a dual-level binary geothermal power plant.* Geothermics, 2002. **31**: p. 709-724.
2. Schuster, A., et al., Energetic and economic investigation of organic Rankine cycle applications. Appl. Therm. Eng., 2002. **29**: p. 1809-1817.
3. Ozturk, H.K., et al., *Energy and exergy analysis of Kizildere Geothermal Power Plant, Turkey.* Energy Sources Part a-Recovery Utilization and Environmental Effects, 2006. **28**(15): p. 1415-1424.
4. Talbi, M. and B. Agnew, Energy recovery from diesel engine exhaust gases for performance enhancement and air conditioning. Appl. Therm. Eng., 2002. **22**: p. 693-702.
5. Camacho, E.F. and C. Bordons, *Model Predictive Control*. Second ed. Advanced Textbooks In Control and Signal Processing, ed. M.J. Grimble and M.A. Johnson. 2004, United States of America: Springer. 405.
6. Casella, F., *Modeling, simulation, control, and optimization of a geothermal power plant.* IEEE Transactions on Energy Conversion, 2004. **19**(1): p. 170-178.
7. Seferlis, P. and M.C. Georgiadis, eds. *The Integration of Process Design and Control*. 2004, Elsevier B. V.: Amsterdam, The Netherlands.
8. Sinnot, R.K., Coulson and Richardson's Chemical Engineering Volume 6 - Chemical Engineering Design. 2005, London, UK: Butterworth-Heinemann Ltd.
9. Gnuteck, Z. and A. Bryszewska-Mazurek, *The thermodynamic analysis of multicycle ORC engine.* Energy, 2001. **26**(1075-1082).
10. Kaplan, U., Advanced Organic Rankine Cycles In Binary Geothermal Power Plants, in World Energy Congress 2007: Rome, Italy.
11. Quoilin, S., et al., *Thermo-economic optimization of waste heat recovery Organic Rankine Cycles.* Applied Thermal Engineering, 2011. **31**(14): p. 2885.
12. Felgner, F., L. Exel, and G. Frey, Component-oriented ORC plant modeling for efficient system design and profitability prediction, 2011, IEEE. p. 196-203.
13. Sun, J. and W. Li, Operation optimization of an organic rankine cycle (ORC) heat recovery power plant. Applied Thermal Engineering, 2011. **31**(11): p. 2032-2041.
14. Zhang, J., et al., Linear active disturbance rejection control of waste heat recovery systems with organic Rankine cycles. Energies, 2012. **5**(12): p. 5111-5125.
15. Zhang, J., et al. Multivariable control of an ORC power plant for utilizing waste heat. in Proceedings - 2012 International Symposium on Computer, Consumer and Control, IS3C 2012. 2012.
16. Jung, H.C. and S. Krumdieck, *Modelling of organic Rankine cycle system and heat exchanger components.* International Journal of Sustainable Energy, 2013: p. 1-18.
17. Ghasemi, H., et al., Modeling and optimization of a binary geothermal power plant. Energy, 2012.
18. Wang, D., et al., Efficiency and optimal performance evaluation of organic rankine cycle for low gread waste heat power generation. Energy, 2013. **50**(1): p. 343-352.
19. Thome, J.R. *Wolverine Heat Transfer Engineering Data Book III: Chapter 8 Condensation Inside Tubes*. 2006 [cited 2013 Web Page]; Available from: http://www.wlv.com/products/databook/db3/data/db3ch8.pdf.
20. Kern, D.Q., *Process heat transfer*. 1950, New York: McGraw-Hill.
21. Law, A.M. and W.D. Kelton, *Simulation Modeling and Analysis*. 1991, New York: McGraw-Hill, Inc.
22. Kleijnen, J.P.C., *Theory and methodology: verification and validation of simulation models.* European Journal of Operational Research, 1995. **82**: p. 145-162.
23. Paez, T.L. *Introduction to model validation*. in *IMAC-XXXVII*. 2009. February 9-12, Orlando, Florida, USA, : Society of Experimental Mechanics Inc. .
24. Sargent, R.G., *Verifying and validating simulation models*, in *1996 Winter Simulation Conference*, J.M. Charnes, et al., Editors. 1996, IEEE: Piscataway, New York. p. 55-64.